

# An investigation of microstructure and tribological performance of the WC-CrCo coating

C. J. SHEN<sup>a,\*</sup>, S. Y. ZHOU<sup>a,b</sup>, H. ZHANG<sup>b</sup>, Z. CHEN<sup>a</sup>, J. ZHOU<sup>a</sup>

<sup>a</sup>*School of Material Science and Engineering, China University of Mining and Technology, Xuzhou, Jiangsu 221008, P.R. China*

<sup>b</sup>*XCMG Excavator Machinery CO. LTD, Xuzhou Jiangsu 221004, P.R. China*

In order to improve the wear resistance of dipper made of AISI 1035, the WC-CrCo coating was sprayed on AISI 1035 by HVOF. Afterwards, the microstructure and tribological performance were evaluated, and the tribological properties and wear mechanisms were mainly investigated in terms of dry friction, lubrication and composite medium. The results showed that the as-sprayed WC-CrCo coating had a homogeneous and dense microstructure, only with little WC decarburization, and the WC-CrCo coating had a great comprehensive property with the  $HV_{0.2}$  is 1391 and the fracture toughness is 3.78 MPa.m<sup>1/2</sup>. Additionally, the wear rate subjected to under dry friction was as small as  $3.87 \times 10^{-8}$  g/Nm, and worn surfaces showed severe lamellar fracture. While wear mechanism under lubricated condition was plastic deformation and abrasive wear. Under composite medium friction, the wear damage was described by the micro-grinding and polishing, and wear mechanism conformed to the corresponding tribo-media. Finally, difference in wear mechanism was explained in terms of the medium interaction.

(Received February 5, 2012; accepted July 10, 2014)

**Keywords:** High velocity oxy-fuel spraying, WC-CrCo, Wear resistance, Friction behavior, Tribo-media

## 1. Introduction

As engineering applications become more demanding, wear resistance of material surface are critical for many machine components in gas/steam turbine, bucket arm and aero engines [1]. Thermal spraying is one of the most widespread used surface treatments, which could ensure the surface wear and corrosion resistance. High Velocity Oxygen Fuel(HVOF) is one of the advanced spray technique with lower levels of carbide decomposition and phase transformation, compared with plasma spraying and detonation gun spraying (DS) [2, 3]. The low temperature and supersonic speed avoid substrate overheat and make it possible to deposit at a relatively low temperature [4].

In order to obtain wear/corrosion-resistant coating with high hardness, the most recommended materials are ceramics and hard metals. Thus, WC-based cermets are used in surfaces of accessories against abrasion, erosion and other forms of damage, owing to its low wear rate, exceptional hardness and environmental friendliness [5, 6]. For cermets coating produced with HVOF, most of investigators focused on the relation among feedstock powder characteristics, process conditions, microstructural parameters and wear performance [7-8]. As reported by Sahrui [4], wear behavior of the cermet coating was controlled by several factors, such as the morphology of spraying powders, size and distribution of carbide particles. Yang et al. [9] have studied the effect of grain size of carbide on the sliding and abrasive wear behaviors of WC-12%Co coatings. It is shown that the WC-Co coating exhibits an extraordinary wear-resistance. Recently, the wear behavior under dry friction was studied and the counterpart was limited to sintered Al<sub>2</sub>O<sub>3</sub> or SiC. In the

present investigation, an attempt has been made to study the dry sliding friction and wear behavior of mild steel (MS) and mild steel coating (MSC) specimens on a pin-on-disc machine [10]. Additionally, microscopic analysis showed that tribofilm plays an important role in the sliding wear. Based on these wear experimental results, the smooth and compact tribofilm, formed in the cermets-based coating, would be caused by the circulation of wear debris where plastic deformation occurs [11, 12]. However, many wear studies, involving HVOF sprayed coatings, are only concentrated on certain single wear condition [13-15]. Stewart et al. have examined the abrasive wear performance by a set number of revolutions of the rubber wheel [14]. The tribological behavior under the dry and wet conditions was evaluated using the pin-on-disc tribometer (ball-on-disc configuration), according to American Society of Testing Materials (ASTM) wear testing standard G-99 [16].

There is no doubt that the single condition cannot evaluate credibly the applicability of the more frequently used surface treatments with respect to different working conditions. The comprehensive study, especially about wear behaviors in different tribo-media, is still in lack. In the present work it is aimed to develop an anti-wear coating working under more harsh conditions.

## 2. Experimental details

### 2.1 Materials and coating fabrication

XY-3200 system from Xinye Spray machinery Company Limited, China was used to prepare HVOF

sprayed coating, which has a built-in mass flow controller for accurate control of flow rate of kerosene and oxygen. WOKA 3603 (WC-CrCo) from Sulzer Metco. Limited was used as feed powder which has a particle size distribution of  $-45$  to  $+25$   $\mu\text{m}$ . The spraying substrates were bright drawn AISI 1035 and were grit blasted using XPBM-1560 grit-blasting machine with  $\text{Al}_2\text{O}_3$  grit of size 24 mesh before spraying. Before the preparation of the WC-CrCo coating, specimens were ultrasonically cleaned in the Industrial acetone for 30 min and thoroughly dried. The thickness was aimed at about 250  $\mu\text{m}$ , and optimized parameters of HVOF spraying are listed in Table 1.

Table 1. Parameters for HVOF spraying.

Parameter	Value
Pressure of kerosene / MPa	1.4
Pressure of oxygen / MPa	0.8
Pressure of nitrogen / MPa	1.7
Flow rate of Pressure of / $\text{L}\cdot\text{h}^{-1}$	21
Spray angle	$90^\circ$
Flow rate of oxygen / $\text{m}^3\cdot\text{h}^{-1}$	40
Feeding rate/ $\text{kg}\cdot\text{h}^{-1}$	1.1
Spraying distance/mm	350

## 2.2 Wear and friction test

In practical applications, coated wear-resistant components have to undergo different work conditions in many cases (e.g., mixed condition of lubrication and hard particles). Therefore, it is very crucial and necessary to analyze and investigate the friction and wear behavior of coatings in different tribo-media. The coated sample of  $\phi 10 \times 8$  mm was tested using the pin-on-disc tribometer, as shown in Fig. 1.

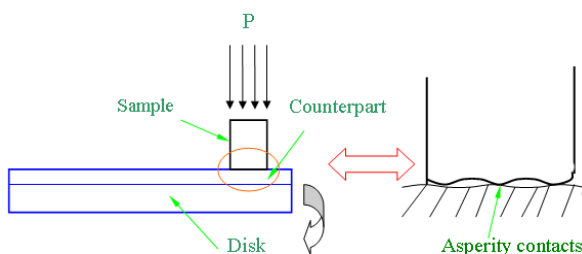


Fig. 1. Schematic of the pin-on-disc friction test.

COF (coefficient of friction) was continuously recorded using a computer. The test conditions are given in Table 2, while, for the composite medium, diamond paste ( $W3.5$   $\mu\text{m}$ ) was selected.

Table 2. Tribological property test conditions.

Parameters	Value
Normal load (N)	20, 35, 70, 100
Wheel (rpm)	250
Relative humidity	25%-35%
Tribological conditions	grease, diamond paste and dry condition
Friction counterpart	Silicon carbide disc, $\phi$ 35mm
Test duration (min)	1000

All samples were ultrasonically cleaned with acetone, dried, and weighed using an electronic weighing balance with an accuracy of 0.01 mg. Mass loss of the coating was measured at every 60 min interval. By measuring mass loss, the wear rate was evaluated after reaching a steady state of wear. The deviation of test data was 10% based on three experiments under the same test condition. All coated samples subjected to wear and friction test were polished using 800 grit emery paper, in order to attain the required surface roughness of  $R_a$  1.6 mm. In each test, at least 100  $\mu\text{m}$  of coatings was left.

## 2.3 Coating characterization

The porosity was determined by image analysis from optical micrographs and observed in three regions of coatings after polished. The micro-Vickers-hardness was tested by HDX-100 hardness tester using a load of 200 g for 15 sec. To avoid the effect of substrates, the cross-section hardness of the WC-based coating was measured, and the cross-sections were cut by using a spark wire cutter. The thickness and porosity of cross-sections were also measured. The bond strength of coatings was measured by using the pull-off test method according to ASTM-C633-2001 standard.

The worn surfaces after ultrasonic cleaned for 15 min were examined by Quanta 250 and XL-30 environmental scanning electron microscopy (ESEM). The XRD patterns of powder materials and as-sprayed coatings were recorded by X-ray diffraction (XRD). W, C, Cr and Co concentrations of the worn surface were conducted by energy dispersive spectroscopy (EDS).

## 3. Experimental results

### 3.1 Microstructure of the coating

The uniformity of melting process, ease of flow from the feeder to the pistol and phase composition was strongly influenced by feedstock powder morphology.

More detailed investigations of the tribological performance as well as the wear track during sliding friction tests were carried out. Fig. 2 showed ESEM micrographs of the powder and as-sprayed surface of HVOF sprayed WC-CrCo coating. The highly porous powder particle had a spherical morphology with a size in the range of 25–45  $\mu\text{m}$ . In microscopic scales, the morphology of the coating in the as-sprayed condition presented a rough and layered microstructure, including some spherical un-melted particles and spongiform inclusion (Fig. 2). Cross-sectional images depicted in Fig. 3a showed a mount formation of the layered structure, accompanied by difficultly deforming of WC-CrCo powders. As shown in Fig. 3b, the WC-CrCo coating was dense with sharp irregular shapes of WC distribute uniformly in the binder phase. This coating had a high carbide volume fraction (more than 80%). Fig. 3c presented elements distribution curves of the cross-section. It could be detected by the diffusion boundary layer that a great diffusion union with the steel substrate occurs. Excellent bonding between WC particles and Co/Cr was also observed in the coating (Fig. 3a). In order to examine the coating microstructure, crystal structures were characterized by X-ray diffraction. It was clarified that initial WC-CrCo powder was composed solely of WC and metallic binder phase Co/Cr, as shown in Fig. 4. In comparison of the feedstock powder, the X-ray diffraction pattern in as-sprayed condition exhibited peaks indexes to a main WC peak, followed by lower intensities of Co/Cr and secondary carbide  $\text{W}_2\text{C}$ . It was confirmed that a quite homogeneous and dense coating with low porosity was prepared [6].

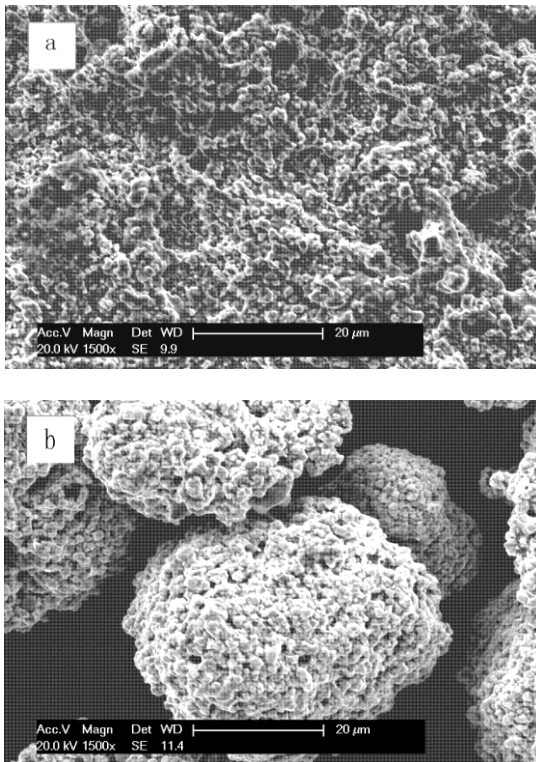


Fig. 2. (a) Powder morphology and (b) as-sprayed surface Morphology of WC-CrCo coating.

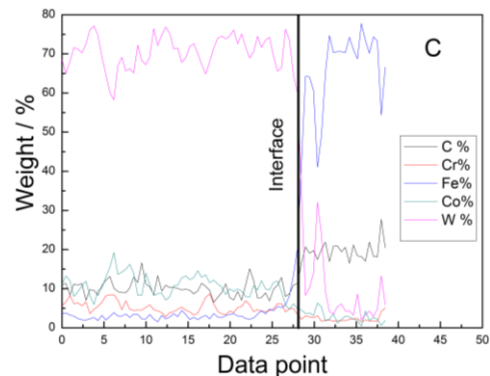
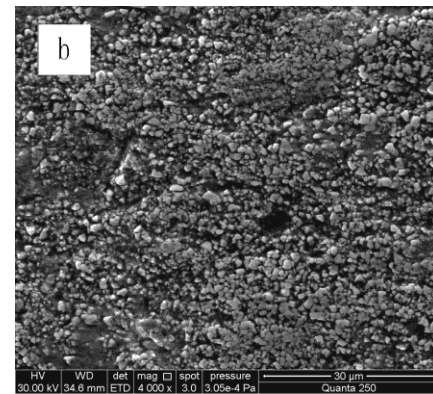
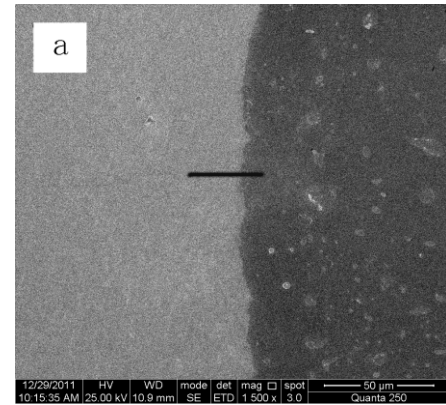


Fig. 3. Morphology of WC-CrCo coating: (a) cross-section, (b) surface after polished and (c) elements distribution of cross-section.

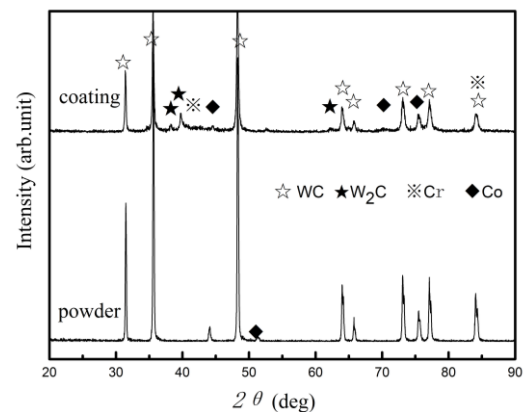


Fig. 4. XRD spectra of WC-CrCo powder and as-sprayed coating.

### 3.2 Tribological properties

Prior to wear test, mechanical properties of the WC-CrCo coating were evaluated (see Table 3). A value larger than  $HV_{0.2}1350$  was detected by micro-hardness

measurements on the coating. The bond strength of the coating can be achieved in the range of 55 MPa. Porosity was 0.86 %, measured using Image-pro-plus analysis software.

Table 3. Results of the coatings characteristics.

Coating	Hardness ( $HV_{0.2}$ )	Porosity	Bond strength (MPa)	Fracture toughness <sup>a</sup> ( $MPa \cdot m^{1/2}$ )
AISI 1035	152	—	—	—
WC-CrCo	1391	0.86%	56.02	3.78

<sup>a</sup> from manufacture's information

In the present work, tribological properties of the WC-CrCo coating in different media were investigated with respect to different working conditions. Fig. 5 showed typical coefficient of friction (COF) versus sliding distance curves under dry, lubrication and composite conditions, and the steady value was 0.462, 0.319 and 0.101, respectively. While the COF curve of the coating lubricated by grease showed a smaller fluctuation than others. Wear rate of the WC-CrCo coating in different tribo-media has been shown in Table 4. It was lubrication effect which led to slight wear damage and provided an excellent anti-wear characteristic. Wear rate of coating lubricated by grease with sliding distance up to 27000 m was  $1.92 \times 10^{-8}$  g/Nm, much less than other tribo-media.

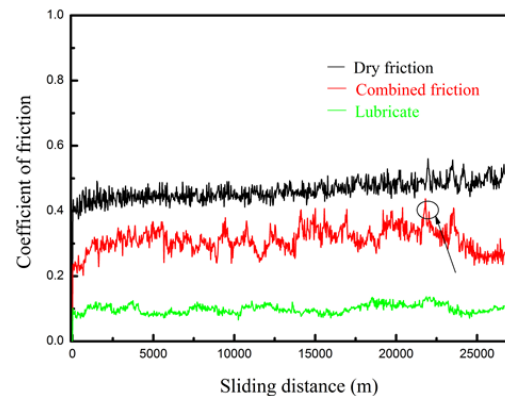


Fig. 5. Evolution of the COF vs. sliding distance under different tribological conditions.

Table 4. Mass loss of WC-CrCo coating under different tribological conditions.

Tribological condition	Mass loss (g)	Wear rate ( $\times 10^{-8}$ g/Nm)
Dry friction	0.02210	3.84
Combined friction	0.05074	9.5
Lubricate by grease	0.01025	1.92

The wear rates and COF for the WC-CrCo coating at different loads have been plotted in Fig. 6. The COF value was in the range of 0.34-0.46 and decreased with increase of the applied load. It was coincident with Picas et al. [17], who showed that the coefficient of friction was about 0.3 for sliding distances up to 144 m, at 30 N under sliding speed of 0.1 m/s against sintered carbide ball. It had a small wear rate of  $2.772 \times 10^{-8}$  g/Nm at a load of 35 N. Measurements at a lower test load are characterized by substantial scatter accomplished by vibrations in the loading arm of the rig. With the increase of applied load (from 35 N to 100 N), it rose up to  $3.046 \times 10^{-8}$  g/Nm. According to previous reports [13, 14, 18], the wear rate of the WC coating is about  $10^{-6}$  mm<sup>3</sup>/Nm, which is almost liner as a function of the load.

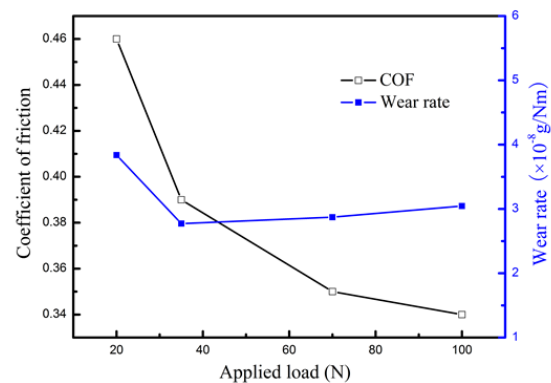


Fig. 6. COF and wear rate vs. applied load of the WC-CrCo coating under dry friction.

### 3.3 Analyses of worn surfaces by ESEM and EDAX

In order to investigate wear behavior under three wear conditions, worn surfaces were studied by ESEM evaluation. Figs. 9-11 showed worn surfaces of HVOF sprayed WC-CrCo coating under different conditions. Apparently, wear track topographies were quite different, which suggested that wear progressed by different mechanisms in different media. Typical aspect of worn surface of the WC-CrCo coating at a 20 N load has been shown in Fig. 7, several grooves, scratches and lamellae fracture can be seen. The wear scars were short and oriented in sliding direction, indicative of brittle fracture. Moreover, some cracks were observed, as shown by arrows in Fig. 7. And the formation of cracks in wear track was followed by pullout of the WC fragments. As shown in Fig. 10, the EDAX analysis revealed that the concentrations of binder phases decreased after worn in comparison with as-sprayed surface, because the binder phases were softer and easier to deform. The above

observations well conformed to the corresponding friction properties under dry friction (section 3.2.2).

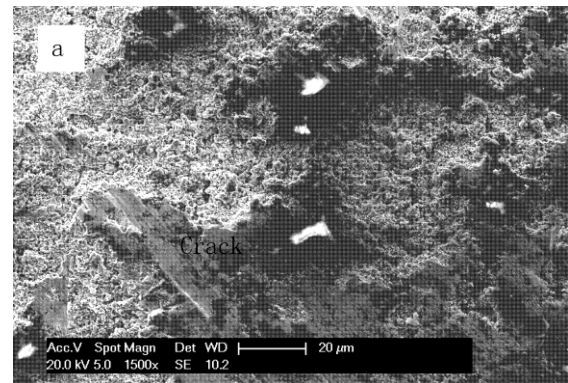


Fig. 7. Worn surface of the WC-CrCo coating after dry friction (25 N applied load).

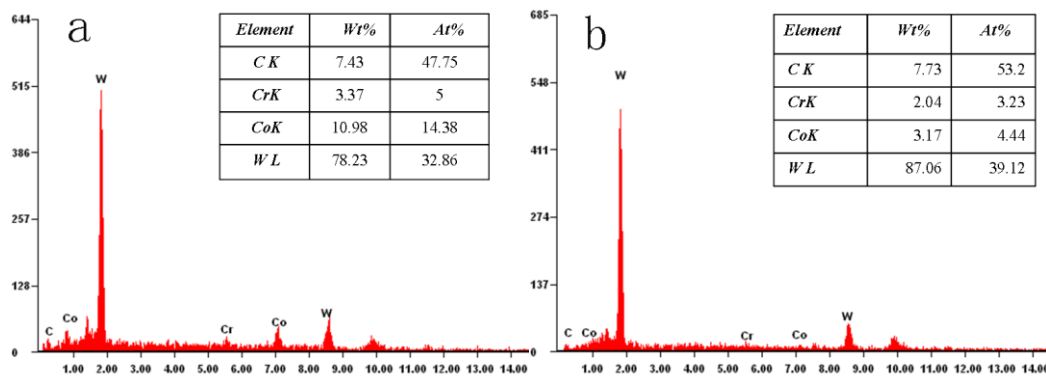


Fig. 8. EDAX analysis spectra of (a) as-sprayed surface and (b) wear scar.

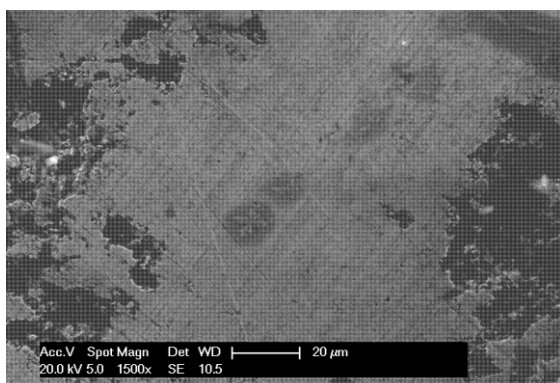


Fig. 9. WC-CrCo coating's wear track under composite friction.

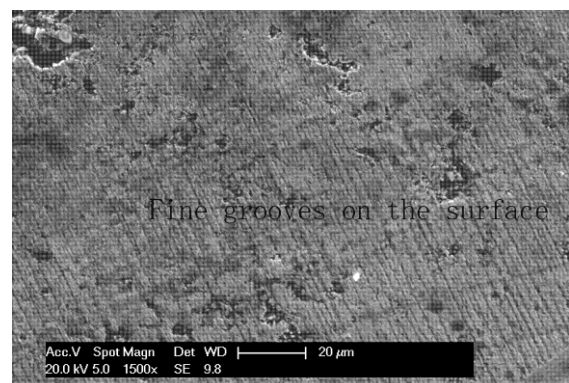


Fig. 10. Wear track of WC-CrCo coatings lubricated by grease.

Compared with dry friction, more detailed analysis subjected to the lubricated and composite media was carried out. The worn surface, without signs of

micro-ploughings (Fig. 9), was comparatively smooth only with some WC which protruding slightly from the substrate removed during the process of grind. Contrarily, some grooves which indicated ploughings and plastic deformation was much more apparent in lubricated condition. It showed much obvious worn trace compared to the composite medium in Fig. 10. In contrast, grease which acted as a lubricant reduced the tribocontact, and subsequently reduced the COF value from 0.462 to 0.101, resulting in a very low wear rate.

## 4. Discussion

### 4.1 Coating microstructures

Detailed description of the microstructure evolution has been given by Stewart [14]. A few salient points, directly relating to mechanic properties and wear resistance, will be analyzed detailedly. The powder particle has a spherical morphology with large holes within it. Thus, this spherical form is idea for feedstock powder since it performs better with respect to deposition rate, and it has lower ratio of volume, liquidity and better multi-directional symmetry which provides a uniform thermal exchange between the flame and particles [19].

The WC-CrCo coating showed a great continuity and adherence in cross-section, as detected by ESEM. The WC-Co coating was formed by piling up of the impacting droplets which were flattened by the acceleration forces and rapidly cooled down [15]. High velocity and momentum of powders compelled plastic deformation in the deposition process, resulting in the enhancement of hardness and wear resistance relatively. On the other hand, the WC-CrCo coating contained a high concentration of WC phase, as shown in Fig. 3b (the higher proportion of gray phase). Fig. 3c presented the diffusion of the W elements in the cross-section of the WC-CrCo coating. The detection of diffusion boundary layer gave the fact that a good diffusion union with the steel substrate formed. Similarly, it can be anticipated that surface microstructure would be beneficial to their excellence in the mechanical and tribological properties.

The XRD spectra of WC-CrCo powder and as-sprayed coating have been shown in Fig. 4. With the present spraying parameters, very compact coating with high control of composition was produced, only with little WC decarburization. Most of WC phase is retained because of the low flame temperature and high particle velocity. In addition, some  $W_2C$  phase has formed during thermal spraying. Similar observation was also made by Yang et al. [20]. Presence of  $W_2C$  in the coating can be attributed to partial decarburization and carbon loss of WC. Cobalt peak is not obvious, which indicates that binder phase has dissolved into some composite phases. These are typically format in the metallic binder phase, which is consistent with the results of Antonio et al. [13], where  $W_2C$  and  $Co_3W$  have been found in the WC-12% Co coating, and the most common transformations are  $WC \rightarrow W_2C$  and  $WC-Co \rightarrow Co_3W_3C$  (brittle and

detrimental).

### 4.2 Tribological performance

It is clear that the WC-CrCo coating behaves differently in relation to COF and wear loss under dry friction, composite and lubricated conditions. As shown in Fig. 5, there is a steady stage that can be observed in COF curves, which reveals a steady course after an initial running-in stage. The steady value is 0.462, 0.319 and 0.101, respectively. After rising stage in the beginning, the value of COF decreased with a small fluctuation, and then increased gradually. In the composite medium, sudden fall can be observed, maybe owing to the detachment of large lamellas (arrows in Fig. 5). The coating has a minimum value of COF lubricated by grease, which shows a smaller fluctuation in COF curves than other media. Obviously, the lowest COF value is the result of lubricating action resulting from the grease. The ductile lubricating film could reduce the shear stress caused by the sliding contact. In the composite medium in which diamond acting as abrasive, coatings is severely damaged. The severity increases due to added diamond in relation to abrasive wear, as a consequence wear rate increases from  $3.84 \times 10^{-8}$  g/Nm to  $9.5 \times 10^{-8}$  g/Nm. This confirms the sensitivity of the tribo-medium to the performance of the coatings. In this case, anti-wear phase maybe removed from the coating surface together with the binder phase. The diamond trapped in contact zone forms a third-body interface, which separates the original sliding interface, decreases the load-supporting capacity and reduces the abrasion resistance. Thus, COF is not only determined by friction of mutual counterparts, but also influenced by the tribo-medium. Therefore, the relationship between the friction and friction resistance is found to be dependent on the tribo-medium, and it also results in different degrees of worn damages. In a word, the WC-CrCo coating, with the wear rate as small as  $3.87 \times 10^{-8}$  g/Nm, could be promising candidate coating for the sliding components subjected to harsh working conditions.

The wear rates and COF for the coating at different loads have been shown in Fig. 6. The COF value decreases from 0.34 to 0.46 with the increase of applied load, due to the increase of contact area. It has a peak value in wear rate ( $3.837 \times 10^{-8}$  g/Nm) at 20 N, possibly due to intrinsic heterogeneities at the initial load. In addition, it has a small wear rate of  $2.772 \times 10^{-8}$  g/Nm at a load of 35 N. With the increase of applied load from 35 N to 100 N, it raises up to  $3.046 \times 10^{-8}$  g/Nm. With the increase of the load, wear rate is almost steady (in the range of the  $10^{-8}$  order of magnitude). WC as a hard phase prevents the coating from seriously worn damage, resulting in a moderate change. According to the theory of friction [18, 21], the friction coefficient  $\mu$  of metals is independent of the load  $L$ . As for ceramics, the coefficient is proportional to  $L^{-1/3}$ . Also, wear loss is liner as a function of the load, and wear loss of the WC-CrCo coating increases significantly with the rise of load [18]. The deviation on wear rate versus load behavior could be

explained by the role of WC phase. The HVOF sprayed WC-CrCo coating exhibits a stability wear resistance at the high and low loads.

### 4.3 Wear mechanism analyses based on tribo-media

Subjected to dry friction, the rough worn surface is caused by a shear fracture typical of severe wear damage. This damage connects with the gradual primary loss of the binder phase from the surfaces, leading to the weakening of the adhesive property of the hard phase and binder phase, and particles pull-out. Therefore, brittle fracture is the predominant mechanism, and still considering the higher severity in relation to gradual primary loss of the binder phase.

The EDAX analysis reveals that the concentration of WC decreases after worn, as shown in Fig. 10. Co and Cr are prone to cause deformation damage. When wear damage occurs, the binder phase is removed and carbide grains sustained by the binder phase automatically come out. This process was also reported by Mindivan [6], who showed that the WC-CrCo coating was worn by an initial cobalt extrusion followed by carbide removal or fracture, resulting in an enrichment of cobalt in the surface.

Based on the analysis of worn traces combined EDAX results, the worn process can be proposed. Firstly, when two surfaces are brought into sliding contact, Cr and Co phases between WC phases undergo severe deformation. Secondly, deformed Cr and Co phases are extruded by the compressive stress of protruding asperities of SiC counterpart. Finally, brittle fracture and pull-out of WC phase occur when the support of the binder phase is no longer present, leading to the original formation of wear debris.

Results of dry friction cannot, however, be generalized to analyze other media. The wear rate and worn traces are used to analyze wear mechanism, though wear rate in composite medium is higher than in lubricated condition. Analyzed results for worn surface are exactly adverse (Figs. 9 and 10). A high stress condition forms in the contact interface by micro-scales abrasive, which appears that a polishing process is acting as indicated by the presence of smooth areas. This interesting phenomenon could be explained that diamond is analogous to medium used in polishing process of the metallographic preparation. As a consequence, wear mechanism could be described as grinding and polishing wears, forming severe three-body wear. According to Zhao [22], polishing was regular mechanism in chemical reaction film, which converted strongly bonded surface molecules, thereby removing surface materials at the molecular scale.

Under lubricated condition, some fine grooving indicates plastic deformation and abrasive wear. Abrasive wear was caused by the asperity of counterpart. As depicted before, the plastic deformation wear is induced by rolling and sliding particles together, resulting in the formation of binder phase. Thus the wear mechanism can be described as the mutual effect of

plastic deformation and abrasive wear.

Based on evidences and observations corresponding to tribological behaviors under different tribo-conditions, conclusions are convinced. The difference in wear mechanism could be explained in terms of medium interaction in the interface, where high stress leads to high levels of plasticity and formation of cracks.

## 5. Conclusions

WC-CrCo coatings were prepared on AISI 1035 substrates using HVOF technique. The tribological property and wear behavior was investigated in terms of different media. The main conclusions are as follows.

(1) Homogeneous and dense microstructures can be produced by HVOF with high control of composition, only with little WC decarburization. The WC-CrCo coating had a great comprehensive property of HV<sub>0.2</sub>1391 and fracture toughness of 3.78 MPa.m<sup>1/2</sup>.

(2) The WC-CrCo coating had a wear rate as small as 3.87×10<sup>-8</sup> g/Nm under dry friction. Relationship between tribological property and wear mechanism was found to be dependent on wear medium, resulting in different degrees of worn damage.

(3) Dry worn surfaces showed severe lamellar fracture, while wear mechanism under lubricated condition was plastic deformation and abrasive wear. In tests with composite medium, the wear damage was dominated by micro-grinding and polishing. The differences in wear mechanism could be explained in terms of the medium interaction.

## Acknowledgment

This work was supported by the specialized research fund for Xugong Construction Machinery Group. The authors are also grateful to the Natural Science Foundation of China (51101169), the Fundamental Research Funds for the Central Universities (2014QNA07) and China Postdoctoral Science Foundation (2013M540475).

## References

- [1] S. Z. Wen, P. Huang, Principle of tribology [M]. Beijing: Tsinghua University Press, 2002.
- [2] J. K. N. Murthy, B. Venkataraman, Surf. Coat. Technol. **2008**, 2642 (2006).
- [3] J. A. Picas, A. Forn, R. Rilla, et al. Surface and Coatings Technology, **204**, 1870 (2010).
- [4] T. Sahraoui, S. Guessasma, M. Ali Jeridane, et al. Materials & Design, **31**(3), 1431 (2010).
- [5] T. Sahraoui, S. Guessasma, N.E. Fenineche, G. Montavon, C. Coddet, Mater. Lett. **58**, 654 (2004).
- [6] Harun Mindivan, Surf. Coat. Technol. **204**, 1870 (2010).
- [7] H. Liao, B. Normand, C. Coddet, Surf. Coat. Technol. **124**, 235 (2000).

- [8] J. Voyer, B. R. Marple, *Wear* **225-229**, 135 (1999).
- [9] Q. Yang, T. Senda, A. Ohmori. *Wear* **254**, 23 (2003).
- [10] V. Rajinikanth, K. Venkateswarlu *Tribology International*, **44**(12), 1711 (2011).
- [11] Q. Yang, T. Senda, A. Hirose, *Surf. Coat. Technol.* **200**, 4208 (2006).
- [12] Z. R. Zhou, *The edge of tribology development* [M].Beijing: Science Press, 2006.
- [13] Antonio Cesar Bozzi, Jose Daniel Biasoli de Mello, *Wear* **233-235**, 575 (1999).
- [14] D. A. Stewart, P. H. Shipway, D. G. McCartney, *Wear* **225-229**, 789 (1999).
- [15] T. Y. Cho, J. H. Yoon, K. S. Kim, *Surf. Coat. Technol.* **202**, 5556 (2008).
- [16] R. J. K. Wood. *Int J Refract Met Hard Mater* **28**, 82 (2010).
- [17] J. A. Picas, Y. Xiong, M. Punset, L. Ajdelsztajn, A. Forn, J. M. Schoenung, *Int J Refract Met Hard Mater.* **27**, 344-9 (2009).
- [18] L. D. Yu, G. W. Shuy, T. Vilaitong, *Surf. Coat. Technol.* **128-129**, 404 (2000).
- [19] E. A. B. Arnoni, A. Lombardi Neto, Rafael Nucci, G. E. Totten, L. C. Casteletti. *Heat treatment*, **23**, 25 (2008).
- [20] Q. Yang, Senda T. Ohmori, *Wear*, **254**(1), 23 (2003).
- [21] S. Houdková, F. Zahálka, M. Kasparová, L. -M. Berger, *Tribo Lett.* **43**, 139 (2011) .
- [22] Y. W. Zhao, L. Chang, S. H. Kim, *Wear*. **254**, 332 (2003).

---

\*Corresponding author: cjshenzx@cumt.edu.cn